DETECTION OF THE WIDE-AREA CRUSTAL MOVEMENT IN KYUSHU USING JERS-1/SAR AND ALOS/PALSAR DATA

PI No:421

Nobuhiro Tomiyama [1], *Katsuaki Koike* [2], *Makoto Omura*[3]

[1] Remote Sensing Technology Center of Japan
[2] Kumamoto University
[3] Kochi Women's University

1. INTRODUCTION

Kyushu Island has the unique geological environments and structures caused by the existences of the edge of Okinawa Trough, wide-area stress fields with normal faults, active volcanoes, terrestrial heat flow and the occurrences of natural hazards like the debris flow and land slide. It is important not only to detect the local deformations caused by the local events but also to measure the accumulation of the small and slow movements in wide region in order to understand the crustal movements of Kyushu region. The differential interferometry of Synthetic Aperture Radar (DInSAR) is the effective tool to estimate the minute topographic changes, but there are a very few applications for the detection of the accumulation of the minute changes in wide region. This study propose a new technical approach for the extraction of wide-area and long-term crustal deformation by DInSAR. Using this technique, the crustal deformation in whole Kyushu in the 1990s was detected using JERS-1 data and it is examined to detect the recent crustal deformation using ALOS PALSAR data.

2. TEST SITE

The test site of this study is whole of Kyushu Island, which is the south west of Japan. Kyushu Island is the third largest island in Japan and it cover about 39900 km^2 of land, stretching about 250 km east-west and 325 km north-south. Fig.1 shows the distributions of active volcanoes and active faults in Kyushu Island. The local movements in Kyushu area were detected by DInSAR in the previous researches [1] [2]. In order to detect the deformation of whole Kyushu Island, a number of scenes of strip-map SAR data, which is called as fine-beam mode for ALOS/PALSAR, are required. In the case of JERS-1/SAR, it is needed 24 scenes to cover whole of island. ALOS/PALSAR can observe earth surface from both of ascending and descending orbits. In the case of ALOS/PALSAR, 22 scenes for ascending and 21 scenes for descending orbit are required respectively. Fig.2, 3, and 4 show JERS-1/SAR and ALOS/PALSAR scene coverage in Kyushu Island respectively. The observation

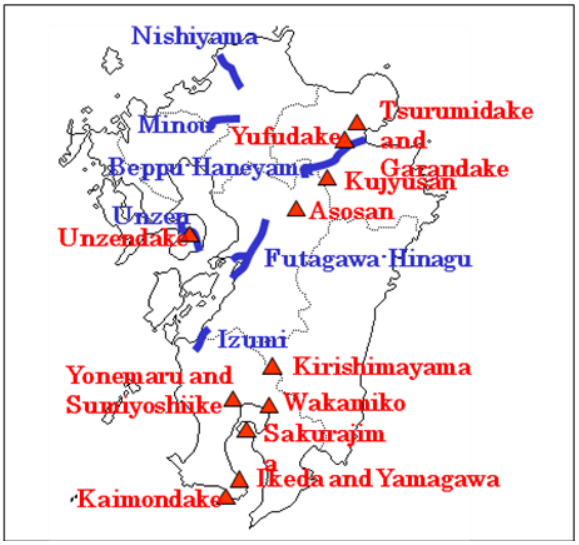

Fig. 1 Main active volcanoes and faults in Kyushu Island

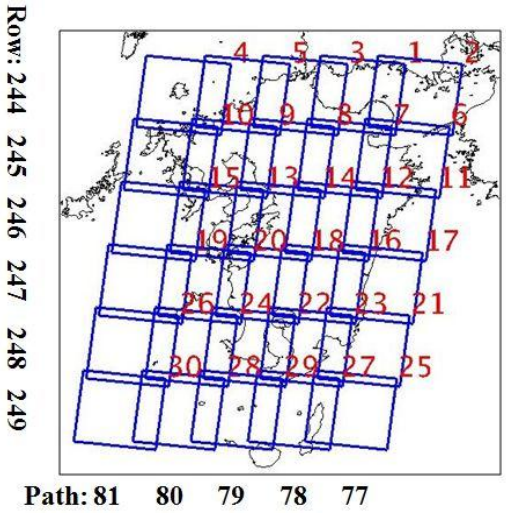

Fig. 2 JERS-1/SAR scene coverage (Descending)

of JERS-1/SAR in ascending orbit was very rare, so the ascending data was not selected for this study.

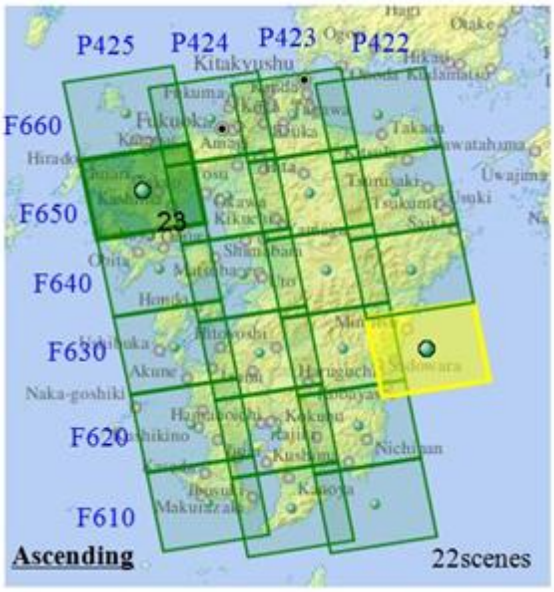

Fig. 3 ALOS/PALSAR scene coverage (Ascending)

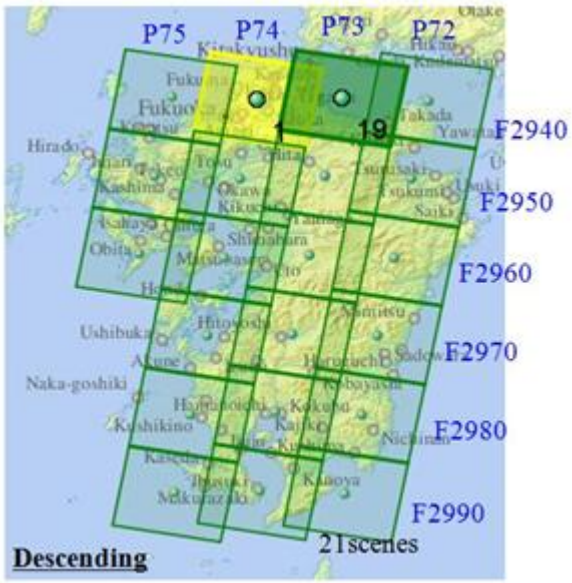

Fig. 4 ALOS/PALSAR scene coverage (Descending)

3. TECHNICAL APROACH FOR ANALYSIS

Usually all scenes in a same path are acquired by SAR in a row. Then a SAR image with connecting all scenes in a same path can be reprocessed at one time. And non-gap interferogram in each path can be detected by DInSAR respectively. But the interferogram at the overlapped region in neighboring two paths has a gap cased by the different off-nadir angle and time difference of two observations. The direction of movement which can be detect by DInSAR depends on off-nadir angle and there are about 2-degree difference of incidence angle between near- range side and far-range side. The time difference

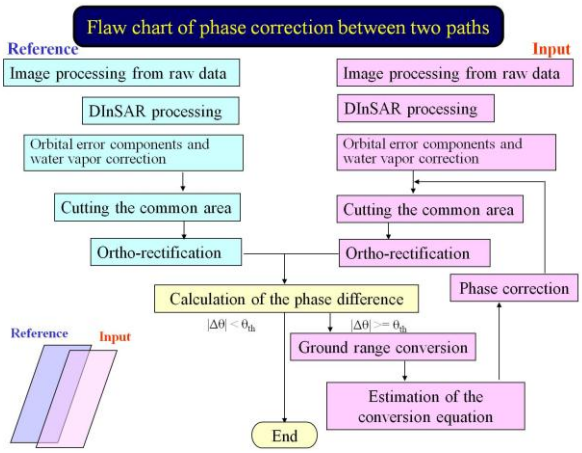

Fig. 5 Flowchart of a new approach of phase correction between two paths

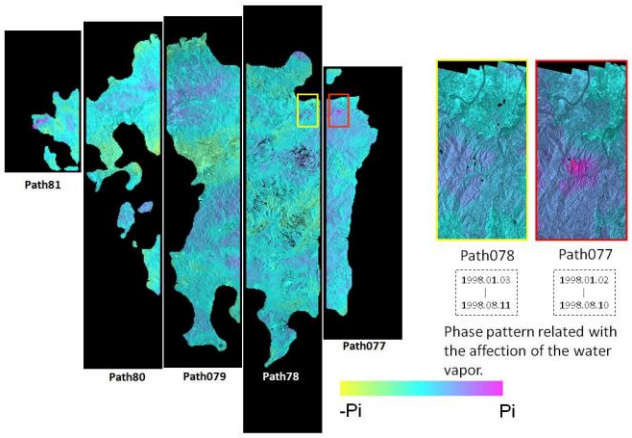

Fig. 6 An example for connection of next door interferogram with phase error correction

often make the difference of amount of displacement. And it leads a different condition of atmosphere delay which is a main cause of error of a interferogram. In order to connect the interferograms of each path, we proposed a new technical approach to connect the neighboring interferograms. Fig.5 shows the flowchart of how to correct the difference of phase between two paths. And using this technical approach, the phase pattern can be modified and it can be connect the interferograms in each path (Fig. 6). JERS-1/SAR observation area shifts to next west path every day. Therefore whole area of Kyushu Island can be observed in only 5 days (between path77 to 88). The short time difference of the observation in each path leads few difference of movement in each path. And the atmospheric conditions in 5 days are able to be assumed almost same except for the case of rainy day. On the other hand, ALOS/PALSAR needs 17 days for next west path's observation. Therefore Time differences are too large and it is difficult to avoid its influence.

4. COMPARISON WITH GPS MEGERMENT

Geographical Survey Institute of Japan (GSI) offers GPS data which is called as "The daily coordinate values of GPS-based control station". Although this GPS data originally indicates the position of GPS station in the Earth Centered Earth Fix Coordinate (ECEF), it can be used to estimate movements by subtractions of coordinate values in different two days. And the number of GPS stations in Kyushu Island is enough to interpolate planar crustal movements. In order to compare with crustal movements which are detected by DInSAR, the values of coordinate should be set to the mean value for the duration of SAR observations for whole Kyushu Island. Hence the mean values in the coordinate of target points for master-observation and slave-observation are set as;

$$M\left(\overline{X}_M,\ \overline{Y}_M,\ \overline{Z}_M\right) \tag{4.1}$$

$$S\left(\overline{X}_S,\ \overline{Y}_S,\ \overline{Z}_S\right) \tag{4.2}$$

The displacements of the GPS station between master and slave observations are;

$$\begin{pmatrix}\Delta X\\ \Delta Y\\ \Delta Z\end{pmatrix}=\begin{pmatrix}\overline{X}_S-\overline{X}_M\\ \overline{Y}_S-\overline{Y}_M\\ \overline{Z}_S-\overline{Z}_M\end{pmatrix} \tag{4.3}$$

The values of position in ECEF coordinates can be converted to the Local North, East, Up (NEU) coordinates by the following equation.

$$P\begin{pmatrix}X_P\\ Y_P\\ Z_P\end{pmatrix}=\begin{pmatrix}(N+H_e)\cos B\cos L\\ (N+H_e)\cos B\sin L\\ \left(N\left(1-e^2\right)+H_e\right)\sin B\end{pmatrix} \tag{4.4}$$

Where, N, H_e, B, L show the radius of prime vertical circle, the ellipsoidal height, latitude, and longitude respectively. The values of movements $(\Delta X,\ \Delta Y,\ \Delta Z)$ in ECEF coordinates are able to be converted to the value of movements $(\Delta X,\ \Delta Y,\ \Delta Z)$ in the local NES coordinates as follows (Fig. 7);

$$\begin{pmatrix}\Delta E\\ \Delta N\\ \Delta H\end{pmatrix}=\begin{pmatrix}0&0&1\\ 0&1&0\\ 1&0&0\end{pmatrix}\begin{pmatrix}-\sin\theta_y&0&\sin\theta_y\\ 0&1&0\\ \cos\theta_y&0&\cos\theta_y\end{pmatrix} \times\begin{pmatrix}\cos L&-\sin L&0\\ \sin L&\cos L&0\\ 0&0&1\end{pmatrix}\begin{pmatrix}\Delta X\\ \Delta Y\\ \Delta Z\end{pmatrix} \tag{4.5}$$

Where

$$\theta_y=\arctan\left(\frac{Z_P}{\sqrt{{X_P}^2+{Y_P}^2}}\right) \tag{4.6}$$

The movement detected by SAR Interferometry is the movement along a line which connects the satellite and target point called as line of sight (LOS). And this movement is a combination of the movements in Range, Azimuth, and Up (Vertical) coordinate. Here, the orientation angle of the path of SAR orbit is set as θ_d, the movements $(\Delta R,\ \Delta Az,\ \Delta H)$ in Azimuth, Range, and Up (AzRU) is calculated by the following equation.

$$\begin{pmatrix}\Delta R\\ \Delta Az\\ \Delta H\end{pmatrix}=\begin{pmatrix}\cos\theta_d&-\sin\theta_d&0\\ \sin\theta_d&\cos\theta_d&0\\ 0&0&1\end{pmatrix}\begin{pmatrix}\Delta N\\ \Delta E\\ \Delta H\end{pmatrix} \tag{4.7}$$

The movement in LOS is calculated by an incident angle θ_{in}, (Fig. 8)

$$\Delta LOS=\Delta R\sin\theta_{in}-\Delta H\cos\theta_{in} \tag{4.8}$$

This equation means that SAR interferometry has no sense for movements along Azimuth direction.

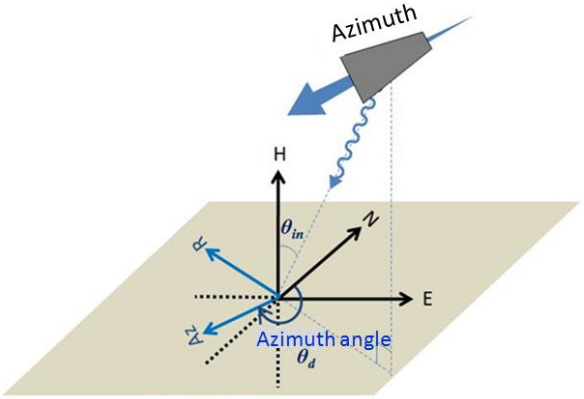

Fig. 7 Coordinate conversion of a movement from NEU to AzRU

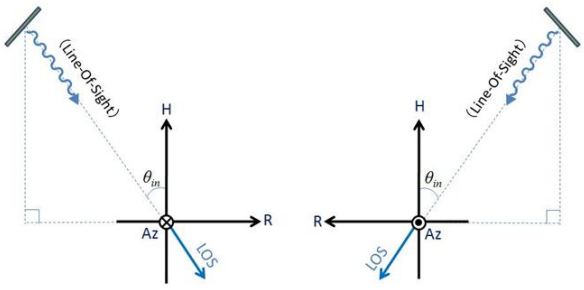

(a) Ascending orbit **(b) Descending orbit**

Fig. 8 Coordinate conversion of a movement from AzRU to LOS

In order to interpolate the movements at any point from the value of the movements at the GPS stations, it is assumed that the value of movement $(\Delta E',\ \Delta N',\ \Delta H')$ at any point is liner to the inverse value of the sum of distance from nearest-surrounding 3 GPS stations' points.

$$\begin{pmatrix}\Delta E'\\ \Delta N'\\ \Delta H'\end{pmatrix}=\frac{\alpha}{d_1}\begin{pmatrix}\Delta E_1\\ \Delta N_1\\ \Delta H_1\end{pmatrix}+\frac{\alpha}{d_2}\begin{pmatrix}\Delta E_2\\ \Delta N_2\\ \Delta N_2\end{pmatrix}+\frac{\alpha}{d_3}\begin{pmatrix}\Delta E_3\\ \Delta N_3\\ \Delta H_3\end{pmatrix} \qquad (4.9)$$

Where

$$\alpha=\frac{1}{\sum_{k=1}^{3}\frac{1}{d_i}} \qquad (4.10)$$

5. DATA PAIRS FOR DINSAR ANALYSIS

One of the most important parameters in order to make high quality of interferogram is the length of base line. The shorter base line is the higher quality of interferogram. In the case of JERS-1/SAR, the length of base line had been preferred less than 1,000m experientially. But there are a few data pairs which can be used for SAR interferometry within this criterion because of low accuracy of orbital information. Additionally for covering whole Kyushu Island, all scenes should be satisfied this criterion. Table 1 shows the list of base lines for all data pair of JERS-1/SAR. There are restrictions to select data pair for DInSAR and few data pair which has long time interval over several years. The data pairs in Table 2 are chosen for this study actually. Comparing with JERS-1/SAR, the quality and accuracy of the orbit information of ALOS/PALSAR are constantly excellent. Therefore there are many candidates for DInSAR analysis using ALOS/PALSAR. Table 3 shows the data pairs of ascending orbit for the analysis.

6. ANALYSIS RESULT

Fig. 9 shows the connected interferograms in Kyushu Island detected by JERS-1/SAR data and this phase pattern is a summation of two interferograms which are Jun. 1996 – Jan. 1998 and Jan. 1998 – Aug. 1998. It is better to select short time interval data pair for reducing the influence of temporal decorrelation. Though other interfergrams of Oct. 1993 – Jan. 1994 and Jan. 1994 – Jun. 1996 were obtained in this study, but these interferograms were not be added in the image of Fig. 9 because GPS information, which is a source of target for comparison about movement, was released since Mar. 1996 [3]. Fig. 10 shows the estimated movement by GPS information since Jun. 1996 to Aug. 1998. The quality of interferogram in Fig. 9 is not so good especially in the mountainous region. But the trend of the interferogram is

Table.1 List of baselines of all combinations for JERS-1/SAR interferometry

Observation Date of Slave data (YYYY/MM) / Observation Date of Master data (YYYY/MM)

Master \ Slave	1992/09	1992/10	1993/01	1993/04	1993/07	1993/09	1993/10	1993/11	1994/01	1996/06	1996/09	1996/10	1997/04	1997/05	1997/11	1998/01	1998/02	1998/03	1998/05	1998/06	1998/08	1998/09	Master
1992/09		× / ×	× / ×	× / ×	× / ×	× / ×	× / ×	× / ×	× / ×	× / ×	× / 1103.77	× / ×	× / ×	× / ×	× / 1428.32	× / ×	× / ×	247.92 / ×	× / ×	× / ×	× / ×	× / 1410.21	1992/09
1992/10			932.23 / ×	643.14 / 1239.16	693.07 / 525.63	× / 552.51	× / ×	× / ×	× / 926.61	× / ×	× / ×	× / ×	× / 697.41	× / ×	× / ×	× / ×	× / ×	× / ×	× / 1279.39	× / ×	× / ×	× / ×	1992/10
1993/01				325.19 / ×	283.97 / ×	× / ×	× / ×	931.33 / ×	× / ×	× / ×	× / ×	× / ×	× / ×	1192.10 / ×	× / ×	× / ×	× / ×	× / ×	× / ×	× / ×	× / ×	× / ×	1993/01
1993/04					49.96 / 743.67	× / ×	× / ×	1123.64 / ×	× / ×	× / ×	× / ×	× / ×	× / ×	1485.18 / ×	× / ×	× / ×	× / ×	× / ×	× / ×	× / ×	× / ×	× / ×	1993/04
1993/07						× / 975.69	× / ×	1074.42 / ×	× / 1339.98	× / ×	× / ×	× / ×	× / 1095.77	1435.85 / ×	× / ×	× / ×	× / ×	× / ×	× / ×	× / ×	× / ×	× / ×	1993/07
1993/09							× / 1221.82	832.16 / ×	1379.18 / 376.01	605.00 / 1093.98	1458.70 / ×	1301.49 / 1465.18	283.08 / 148.29	489.26 / 1255.13	× / ×	1045.10 / ×	× / ×	× / ×	1026.94 / 893.81	474.36 / ×	1083.96 / ×	× / ×	1993/09
1993/10								× / ×	242.98 / 869.30	1087.80 / 239.58	198.34 / ×	317.78 / 270.63	1346.06 / 1109.62	× / 80.57	1320.36 / ×	948.89 / 870.00	749.06 / 1171.73	× / ×	840.32 / 672.84	× / 688.69	770.97 / 850.05	484.26 / ×	1993/10
1993/11									× / ×	× / ×	× / ×	1433.96 / ×	1087.05 / ×	361.92 / ×	× / ×	× / ×	× / ×	× / ×	× / ×	850.5 / ×	× / ×	× / ×	1993/11
1994/01										825.21 / 778.47	235.89 / ×	202.50 / 1125.85	1116.48 / 244.19	× / 894.18	× / ×	857.14 / ×	970.75 / ×	× / ×	735.66 / 711.26	× / ×	677.35 / ×	675.95 / ×	1994/01
1996/06											866.41 / ×	713.49 / 387.15	418.44 / 1002.08	1093.89 / 318.22	× / ×	522.10 / 862.32	× / 1222.25	× / ×	460.70 / 436.20	809.31 / ×	502.83 / 890.28	1231.91 / ×	1996/06
1996/09												158.89 / ×	1217.63 / ×	× / ×	1393.26 / 590.93	750.87 / 1471.79	770.09 / 1068.25	× / ×	643.98 / ×	× / ×	573.70 / 1340.04	457.15 / 430.69	1996/09
1996/10													1058.84 / 1361.56	× / 290.12	× / ×	662.76 / 618.79	639.59 / 901.28	× / ×	544.88 / 789.93	× / ×	482.13 / 582.13	599.07 / 1489.09	1996/10
1997/04														728.70 / 1137.16	× / ×	927.06 / ×	× / ×	× / ×	877.62 / 857.76	701.39 / ×	921.36 / ×	× / ×	1997/04
1997/05															× / ×	× / 906.03	× / 1185.53	× / ×	× / 748.37	658.04 / ×	× / 871.25	× / ×	1997/05
1997/11																× / 1265.68	659.13 / 694.92	1320.83 / ×	× / ×	× / ×	× / 1024.10	980.29 / 217.18	1997/11
1998/01																	1223.56 / 415.34	× / ×	125.34 / 1074.60	1038.09 / ×	180.40 / 173.71	931.77 / 1096.16	1998/01
1998/02																		× / ×	1178.22 / 1481.76	× / 547.44	1107.69 / 332.02	326.87 / 681.27	1998/02
1998/03																			× / ×	× / ×	× / ×	× / ×	1998/03
1998/05																				1076.79 / 938.21	74.73 / 1162.73	872.25 / ×	1998/05
1998/06																					1149.05 / 225.07	× / 1213.07	1998/06
1998/08																						799.33 / 988.28	1998/08
1998/09																							1998/09

Upper: Perpendicular component of base Line (B_{perp}) [m]
Lower: Pelarel component of base Line (B_{para}) [m]

Low probability of Interference (B_{perp} >> 1,000m)

Middle probability of Interference (B_{perp} is near to 1,000m)

High probability of Interference (B_{perp} << 1,000m)

×: Length of baseline is over 2,000m

Tabole.2 Data pairs of JERS-1/SAR Interferometry

Pair No.	Master	Slave	Interval[days]	Baseline length (parp.)[m]	Baseline length (para.)[m]
1	Oct-93	Jan-94	88	796	995
2	Jan-94	Jun-96	880	5	-120
3	Jun-96	Jan-98	572	-617	-470
4	Jan-98	Aug-98	220	-64	0.340

GEONET(over Mar-1996)

Table.3 Data pairs of ALOS/PALSAR Interferometry

Pair No.	Orbit	Master	Slave	Interval[days]	Baseline length [m] Para.	Perp.
1	Ascending	Cycle-12	Cycle-13	44	-125.0	616.8
2		Cycle-13	Cycle-14	44	-150.0	-526.3
3		Cycle-14	Cycle-17	133	51.3	30.4
4		Cycle-17	Cycle-37	880	-150.2	-303.1

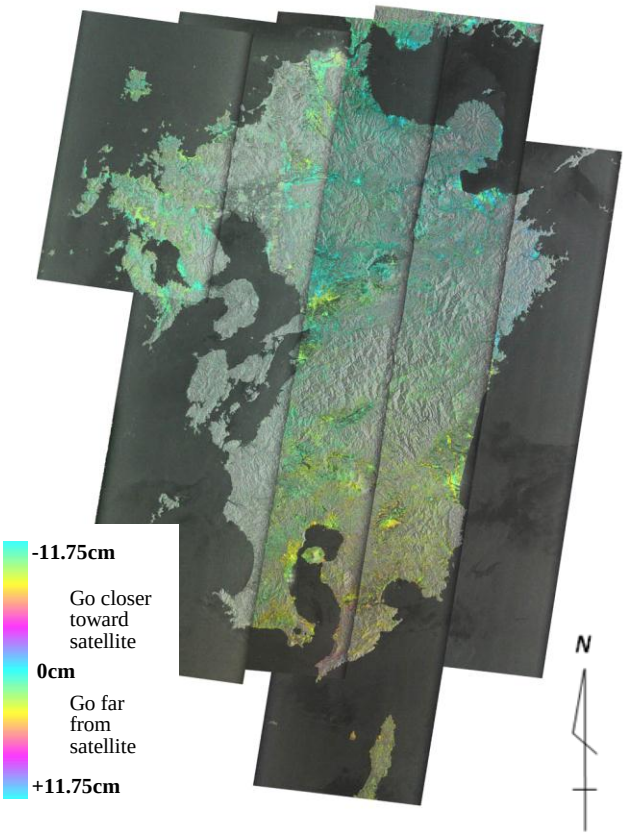

Fig. 9 Result of JERS-1/SAR Interferometry between Jun. 1996 and Aug. 1998.

quite similar to the pattern of △LOS estimated by GPS data in Fig. 10(e). In the east part of Kagoshima prefecture, which is the south-east part of Kyushu, the pattern of inteferogram indicates the movement which is going far from satellite position.

The interferogram obtained by ALOS/PALSAR data in Fig. 11. It indicates the movement between Jan. 2008 – Aug. 2010. And Fig. 12 shows the estimated movement by GPS in same period. The quality of interferogram is higher than that of JERS-1/SAR in Fig. 9, especially in the mountainous reasons. On the other hand, the continuity of interferogram between two paths looks obscure and several local fringe patterns are seen. One of the possible reasons of these results is an influence of the long time differences each-path observation. And it tally take 51 days to cover whole Kyushu Island with 4 paths. Therefore the climate conditions, especially atmospheric conditions are quite different for each-path observations. The orbit of JERS-1/SAR is more suitable for the detection of wide-area crustal movements.

8. SAMMARY

In This study, a new approach to connect the interferograms in different paths for detecting the wide-area and long-term minute crustal movement is proposed. And the possibility of this technique is proved by the

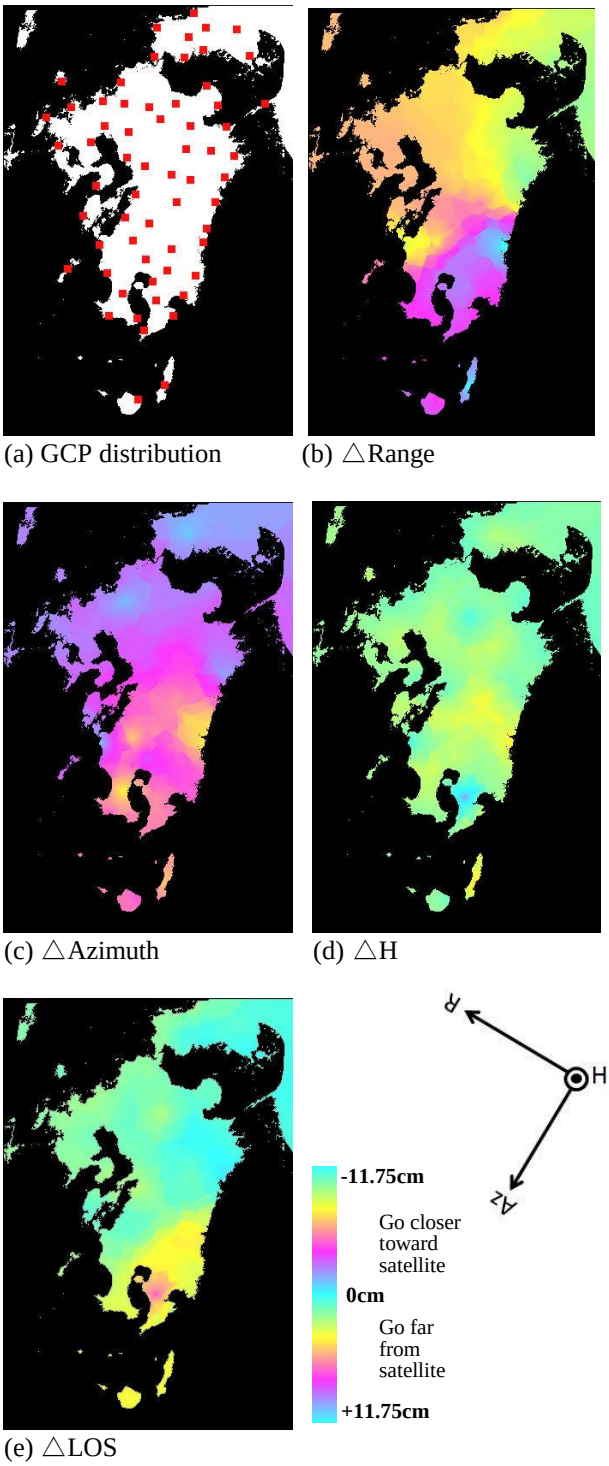

Start: 1996 Jun. 9-13 (mean of 5 days)
End: 1998 Aug.10-14 (mean of 5days)
GPS numbers: 62
Incidence angle: 39.08 [deg]
Azimuth angle: -170.05 [deg]

Fig. 10 Estimated crustal movement by GPS information between Jun. 1996 and Aug. 1998.

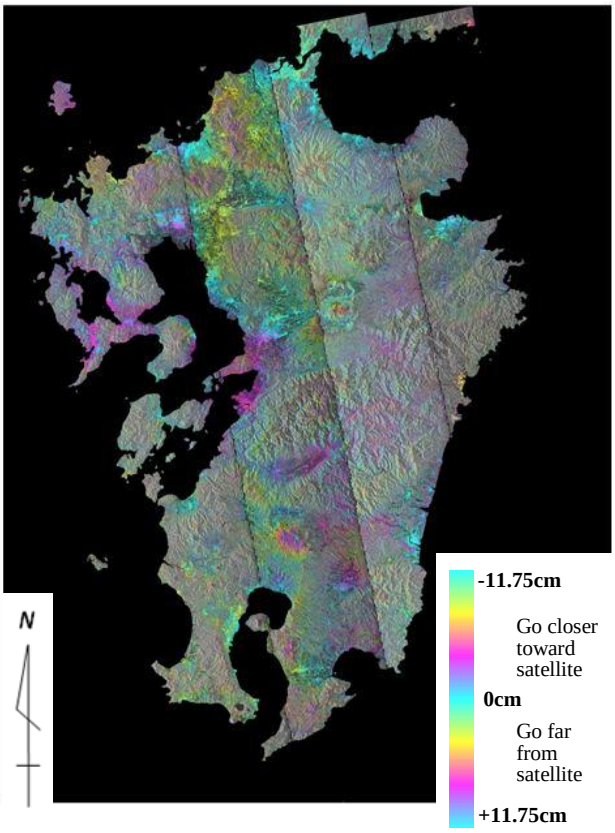

Fig. 11 Result of ALOS/PALSAR Interferometry between Jan. 2008 and Aug. 2010.

analysis using JERS-1/SAR data and ALOS/PALSAR data. Recently, thanks to the advance in technique of DInSAR analysis, ScanSAR Interferometry can be possible for the detection of the wide-area crustal movement. But the pixel resolution of ScanSAR data is not enough to detect the local small changes. And the number of the observation by ScanSAR mode is very poor comparing with that of standard strip map mode. Therefore it is important to detect the wide-area crustal deformation by ordinary interferometry using strip map data and this approach will be of assistance.

9. REFERENCES

[1] Tomiyama N., Koike K., Iguchi M., and Omura M., "Analysis of Topographic Change at Mount Sakurajima, South Kyushu, Japan, Using JERS-1 SAR Interfeorometry, Geoinformatics, vol.22, no. 1, 2011.
[2] Tomiyama N., Koike K., and Omura M., "Detection of Topographic Changes Accompanied with Volcanic Activities of Mt. Hossho by D-InSAR", Advances in Space Research, vol. 33, no. 3, pp. 279-283, 2002.
[3] Tomiyama N., "Detection of Volcanic Crustal Deformation and Wide-area Crustal Movement by DInSAR", Kumamoto University, Ph.D. thesis, pp.69-86, 2011.

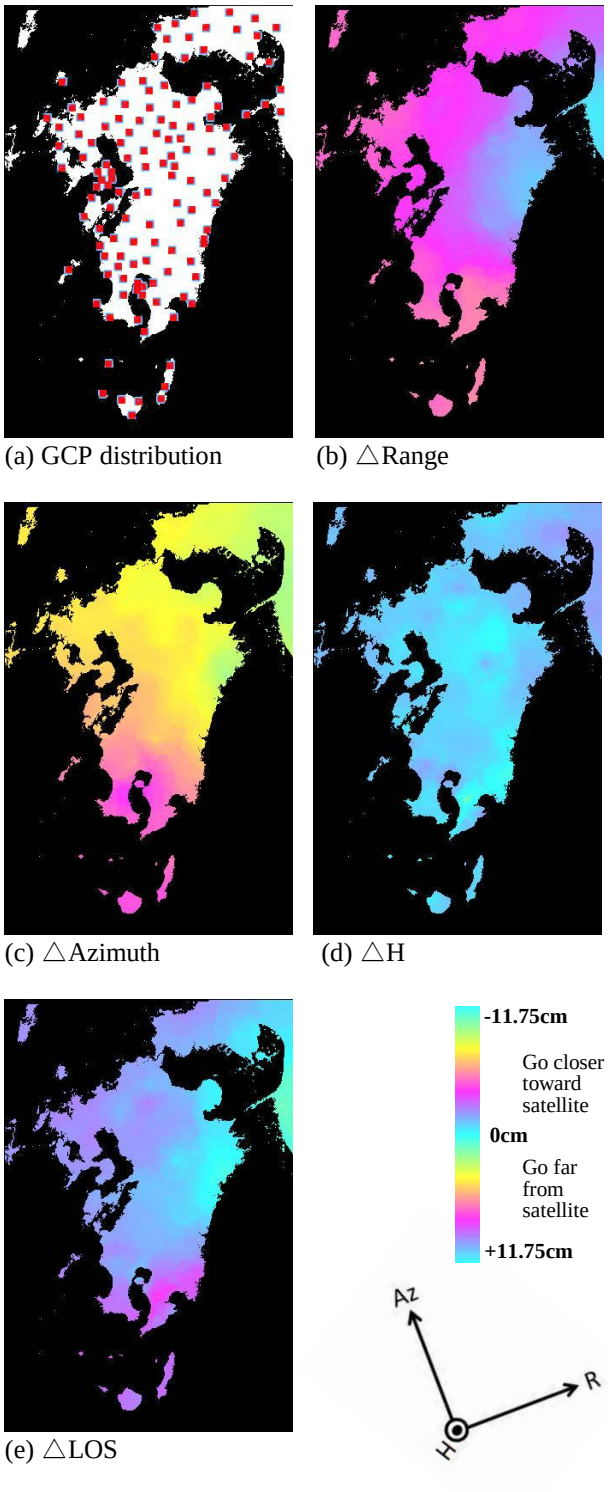

Start: 2008 Jan. 26 – Feb. 29 (mean of 34 days)
End: 2010 Aug. 3 – Sep. 3 (mean of 34 days)
GPS numbers: 129
Incidence angle: 38.73 [deg]
Azimuth angle: -10.22 [deg]

Fig. 12 Estimated crustal movement by GPS information between Jan. 2008 and Aug. 2010.